1.0 nm for Ag^+ and R = 1.5 nm for NO_3^- (Figures 7 and 9).

To obtain similar r_W/r values for CrO_4^{2-} required the reaction radius to be 3 nm.

Thus the scavengers that have a repulsive Coulombic interaction with the electron react at greater distances than do those with an attractive Coulombic interaction.

Energies of Activation. Generally the negative ions in the present study have energies of activation lower than those of positive ions. The negative ions NO_3^- and CrO_4^{2-} are large compared to the positive ions Ag^+ and Cu^{2+}. Both negative ions act as structure breakers (decreasing η), while the positive ions act as structure makers (increasing η).[15]

The energies of activation in pure water are in the order $Ag^+ > Cu^{2+}$ for positive ions and $CrO_4^{2-} > NO_3^-$ for negative ions (Figure 10). Thus the charge effects are manifested as energies and entropies of activation (Table I). When the ions are positive, there is greater attractive Coulombic interaction between the electron and the ion with the larger charge; Cu^{2+} has a larger charge than Ag^+ and has a lower E_2 value. Of the negative ions CrO_4^{2-} has a greater repulsive Coulombic interaction with the electron and thus the energy of activation is higher than for NO_3^-.

In alcohol/water mixtures the E_2 values for reaction with Ag^+ decreases in zone a, are constant in zone b, and decrease in zones c and d. Similar composition dependence is displayed for the reaction with the nitrobenzene molecule.[2] Since these reactions are nearly diffusion controlled, the E_2 values correlate with energy of activation for viscous flow E_η.[2]

The values of E_2 in alcohol/water mixtures for the reaction with negative ions display similar composition dependence in zones c and d (Figure 10). But in zone b, the E_2 values increase with decreasing water content. This region corresponds to a relatively low dielectric constant of the solvent and consequently to a greater repulsive interaction between the electron and the scavenger. The energy barrier for close approach is manifested as larger energies of activation.

Registry No. Ag^+, 14701-21-4; Cu^{2+}, 15158-11-9; NO_3^-, 14797-55-8; CrO_4^{2-}, 13907-45-4; nitrobenzene, 98-95-3.

Time-Resolved Tunable Diode Laser Detection of Products of the Infrared Multiphoton Dissociation of Hexafluoroacetone: A Line-Strength and Band-Strength Measurement for CF_3

J. J. Orlando and D. R. Smith*

Department of Chemistry, McMaster University, 1280 Main Street West, Hamilton, Ontario, Canada L8S 4K1
(Received: September 28, 1987; In Final Form: February 11, 1988)

This paper describes the time-resolved detection of CF_3, C_2F_6, and CO following the infrared multiphoton dissociation of hexafluoroacetone. The primary photolysis mechanism has been established as follows: $(CF_3)_2CO \rightarrow 2CF_3 + CO$; $2CF_3 \rightarrow C_2F_6$. Determination of the CO and C_2F_6 formed in a single photolysis pulse leads to a measure of an infrared line strength and ν_3 band strength for CF_3. Quantification of the CF_3 in this manner allows a study of its reaction kinetics. The reactions of CF_3 with added O_2 and NO were found to have third-body rate constants of $(2.1 \pm 0.5) \times 10^{-29}$ and $(2.8 \pm 0.7) \times 10^{-29}$ cm^6 $molecule^{-2}$ s^{-1}, respectively, at room temperature in the presence of 600 mTorr of hexafluoroacetone.

Introduction

The infrared multiphoton dissociation (IRMPD) of hexafluoroacetone (hfa) was first realized in the late 1970s[1] and subsequent studies showed that the process could be made isotopically selective for ^{13}C and ^{18}O.[2-4] While other reports[5,6] on IRMPD of hfa have appeared in the literature, the primary photolysis mechanism has not been firmly established, although a free radical mechanism is suggested by the products of IRMPD of pentafluoroacetone observed by Drouin et al.[7] In this paper, the dissociation products of hexafluoroacetone (CF_3, CO, and C_2F_6) are detected by infrared tunable diode laser (TLD) kinetic spectroscopy within 25 μs following the photolysis laser pulse. In addition, absolute determination of the C_2F_6 and CO formed in the photolysis pulse enables the quantification of CF_3 and thus a measure of an infrared line strength and band strength for CF_3 ν_3. TLD absorption spectroscopy has previously been used in free radical studies to determine the line strength and band strength of CN,[8] HO_2,[9] and CF_2.[10] Finally, the kinetics of CF_3 decay following the photolysis pulse are examined both in pure hfa and in the presence of added O_2 and NO.

Experimental Section

Our TLD transient detection scheme has previously been described in detail for the detection of CF_2,[11] and a more recent publication describing CF_3 detection has followed.[12] Briefly, the precursor hfa is flowed through a capillary cell (15 cm in length and 1 mm in diameter). The synchronized TLD beam and TEA CO_2 photolysis beam (operating on 10R(10) at 969.15 cm^{-1} with fluences in the capillary ranging from 10 to 35 J cm^{-2}) are made

(1) Hackett, P. A.; Gauthier, M.; Willis, C. *J. Chem. Phys.* **1978**, *69*, 2924.
(2) Hackett, P. A.; Gauthier, M.; Willis, C.; Pilon, R. *J. Chem. Phys.* **1979**, *71*, 546.
(3) Hackett, P. A.; Willis, C.; Gauthier, M. *J. Chem. Phys.* **1979**, *71*, 2682.
(4) Hackett, P. A.; Gauthier, M.; Nip, W. S.; Willis, C. *J. Phys. Chem.* **1981**, *85*, 1147.
(5) Avatkov, O. N.; Aslanidi, E. B.; Bakhtadze, A. B.; Zainullin, R. I.; Turishchev, Yu. S. *Sov. J. Quantum Electron. (Engl. Transl.)* **1979**, *9*, 232.
(6) Fuss, W.; Kompa, K. L.; Tablas, F. M. G. *Faraday Discuss.* **1979**, *67*, 180.
(7) Drouin, M.; Hackett, P. A.; Willis, C.; Gauthier, M. *Can. J. Chem.* **1979**, *57*, 3053.
(8) Balla, R. J.; Pasernack, L. *J. Phys. Chem.* **1987**, *91*, 73.
(9) Buchanan, J. W.; Thrush, B. A.; Tyndall, G. S. *Chem. Phys. Lett.* **1983**, *103*, 167.
(10) Orlando, J. J.; Reid, J.; Smith, D. R. *Chem. Phys. Lett.* **1987**, *141*, 423.
(11) Beckwith, P. H.; Brown, C. E.; Danagher, D.; Reid, J.; Smith, D. R. *Appl. Opt.* **1987**, *26*, 2643.
(12) Brown, C. E.; Orlando, J. J.; Reid, J.; Smith, D. R. *Chem. Phys. Lett.* **1987**, *142*, 213.

0022-3654/88/2092-5147$01.50/0

collinear and focused into the capillary cell. After traversing the cell, the two beams are separated on a diffraction grating, and the TLD probe is focused onto a fast response time (400 ns) infrared detector. The TLD frequency is modulated at 40 kHz back and forth across an absorption feature of either CF_3, CO, or C_2F_6. The detector signal (a measure of the IR transmission of the TLD beam through the capillary as a function of time) is collected on a digital storage oscilloscope, and the signal averaged for 32 CO_2 laser pulses. A background signal (with the CO_2 laser beam blocked) is also collected. Both signals are transferred to a IBM PC, where background subtraction is performed. CO is detected on the P(23) line at 2046.277 cm^{-1} and quantified by using known line-strength data.[13] C_2F_6 was detected near 1263 cm^{-1}, and quantified by plotting α_0, the absorption coefficient per centimeter at line center, versus pressure for standard C_2F_6 samples of known pressure. (Calibrations were not done in the presence of hfa since sample pressures were less than 1 Torr, where no pressure broadening effects are observed.) CF_3 was detected on the $^rR_{16}(20)$ absorption line at 1264.739 cm^{-1}.[14]

Stable product analysis is done by Fourier transform and TLD IR absorption spectroscopy. For this purpose, irradiations are performed in a conventional Pyrex photolysis cell (10 cm in length and 2.5 cm in diameter) into which a TEA CO_2 laser beam is focused by a 25-cm focal length BaF_2 lens. CO_2 laser beam energy measurements are made with a Gentec ED-500 joule meter, and the size of the beam at the focus is determined from the burn spot on thermal paper. Irradiations were again performed by using the 10R(10) CO_2 laser line, with peak focal fluences in the range 3–16 J cm^{-2}.

Results and Discussion

Dissociation Mechanism. There appears to be only one report in the literature regarding the thermolysis of hfa.[15] In that work, the authors report two primary dissociation mechanisms:

$$(CF_3)_2CO \rightarrow CF_3COF + CF_2 \quad (1)$$

$$\rightarrow C_2F_6 + CO \quad (2)$$

with the first reaction dominating at high temperature (above 850 K) and the second dominating at lower temperatures. The low preexponential factor ($10^{9.6}$) determined for k_2 led to the conclusion that reaction 2 proceeded via direct elimination of C_2F_6 rather than via the sequential production of two CF_3 molecules (eq 3), which then combine to form C_2F_6 (eq 4):

$$(CF_3)_2CO \rightarrow CF_3CO + CF_3 \quad (3a)$$

$$CF_3CO \rightarrow CF_3 + CO \quad (3b)$$

$$2CF_3 \xrightarrow{M} C_2F_6 \quad (4)$$

In contrast, the photolysis of $(CF_3)_2CO$ in both the near UV[16] and the vacuum UV[17] has been shown to occur via the reaction pathway (3) and (4). To the best of our knowledge, none of the IRMPD studies conducted to date[1-6] has confirmed whether the dissociation of hfa occurs via direct production of C_2F_6 or via successive elimination of two CF_3 molecules, though the products of IRMPD of pentafluoroacetone do suggest a free radical mechanism.[7] Thus, the first step in our study was to determine the IRMPD mechanism.

Preliminary experiments were carried out by irradiating 1 Torr of hfa in standard photolysis cells at peak CO_2 laser fluences (at the focus) ranging from 3 to 16 J cm^{-2}. FT-IR analysis showed the presence of C_2F_6, and an absorption feature at 1896 cm^{-1} was assigned to CF_3COF. TLD absorption spectroscopy confirmed the presence of CO and C_2F_6 and also showed evidence for some

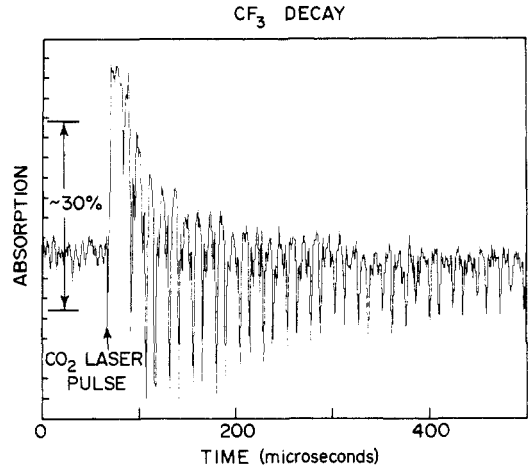

Figure 1. Transient tunable diode laser absorption signal from CF_3 created in the IRMPD of 600 mTorr of hfa in a 1-mm capillary cell at a fluence of 35 J cm^{-2}. Each modulation cycle (40 kHz) scans through the absorption feature ($^rR_{16}(20)$) at 1264.739 cm^{-1} twice, giving a pattern of pairs of peaks.

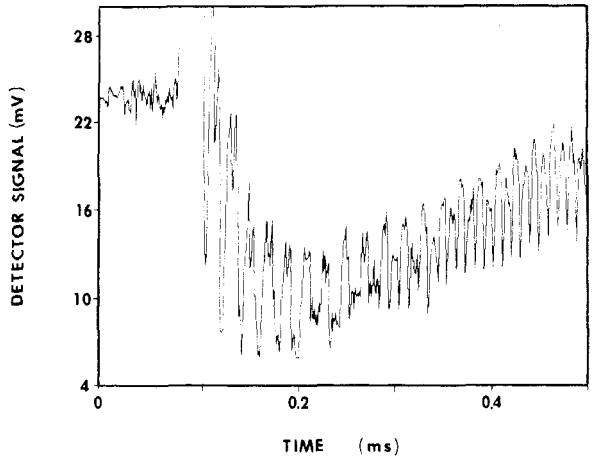

Figure 2. Transient absorption near 1263 cm^{-1} immediately following the photolysis of 600 mTorr of hfa at a fluence of 35 J cm^{-2} in a 1-mm capillary cell. The signal shows CF_3 decay initially and C_2F_6 growth at later time.

C_2F_4. The yield of C_2F_4 relative to C_2F_6 was always less than 10% over the fluence range studied and did not seem to indicate any trend with fluence. These observations led to the conclusion that the main dissociation channel involved (as expected) the formation of C_2F_6 via reaction 2 and/or 3 while a minor channel (less than 10%) led to the production of CF_2 and CF_3COF (reaction 1). Addition of H_2 to the photolysis mixture led to the production of small amounts of CHF_3, suggesting that CF_3 production was occurring.

To distinguish conclusively between reactions 2 and 3, we set out to detect CF_3 using time-resolved TLD absorption spectroscopy[12] in the capillary cell setup described in the Experimental Section. Figure 1 shows that CF_3 is indeed formed following the IRMPD of hfa. Initial (peak) CF_3 yields were varied by a factor of 5 by varying hfa pressure or laser fluence. Typically, about 5–10% of the hfa is dissociated. In 15 separate cases, the product of peak yield times initial half-life is constant to ±10%. Therefore the CF_3 decay is second order, consistent with reaction 4, and wall effects are too slow to contribute significantly. Further, it was shown (see Figure 2) that no C_2F_6 is present immediately following the pulse but that the concentration of C_2F_6 increases with time following the pulse. (The time dependence of C_2F_6 growth is difficult to measure quantitatively because of the interference of CF_3 absorption at early time as seen in Figure 2.) Thus, it seems certain that the IRMPD of hexafluoroacetone predominantly involves the initial production of CF_3 (reaction 3), followed by combination of CF_3 to form C_2F_6 (reaction 4).

(13) Rothman, L. S. *Appl. Opt.* **1980**, *20*, 791.
(14) Yamada, C.; Hirota, E. *J. Chem. Phys.* **1983**, *78*, 1703.
(15) Batey, C.; Trenwith, A. B. *J. Chem. Soc.* **1961**, 1388.
(16) Whytock, D. A.; Kutschke, K. O. *Proc. R. Soc. London, A* **1968**, *306*, 503.
(17) Perkins, G. G.; Austin, E. R.; Lampe, F. W. *J. Chem. Phys.* **1978**, *68*, 4357.

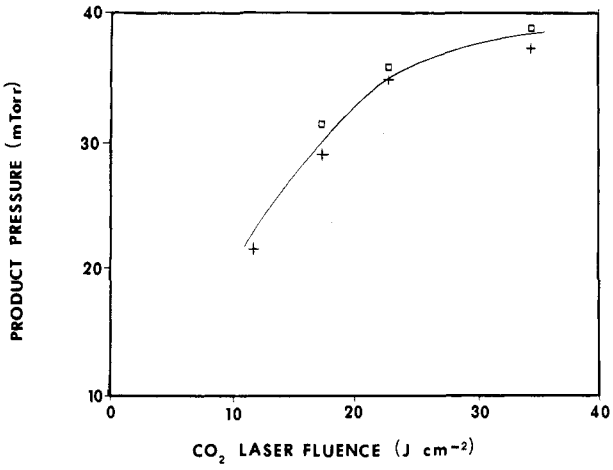

Figure 3. CO (+) and C_2F_6 (□) yield from IRMPD of 600 mTorr of hfa in a 1-mm capillary cell as a function of CO_2 laser fluence.

A search was also made for CF_3, CF_4, and COF_2 by using the transient TLD technique. No evidence of CF_2 or CF_4 was found, indicating that less than about 2 mTorr of each of these species was formed after a CO_2 laser pulse, even at the highest fluences used (35 J cm^{-2}). This would indicate that secondary dissociation of CF_3 radicals to CF_2 and disproportionation of two CF_3 radicals to form CF_2 and CF_4 are unimportant mechanisms for CF_3 decay. Also, it confirms our conclusion above, based on less than 10% C_2F_4 to C_2F_6 yield ratio, that reaction 1 may be neglected under these conditions. Trace amounts of COF_2 (less than 5 mTorr per pulse) were noted, probably the result of CF_3 reactions with the Pyrex walls of the cell, though we cannot rule out the possibility of a very low yield of F atoms, which may etch the wall.

From the stoichiometry of reactions 3 and 4, it is apparent that each dissociation of hfa produces one molecule of CO and two molecules of CF_3 that combine (over a time scale of 400–500 μs) to form one molecule of C_2F_6. Thus, from a measurement of the CO yield 100 μs after the laser pulse and the C_2F_6 yield about 500 μs after the laser pulse in one-pulse photolysis of hfa, it is possible to quantify the CF_3 and thus obtain its infrared absorption line strength and band strength.

Vibrational Relaxation of CF_3. It is important that the CF_3 be vibrationally and rotationally thermalized following photolysis, since detection is done in the vibrational ground state. The increase in the CF_3 absorption signal over the first 50 μs following the CO_2 laser pulse (see Figure 1) is attributed to cascading from vibrationally excited states and/or to collisionally induced dissociation occurring after the pulse. Since CF_3 has a vibrational energy level coincident with the parent hfa (near 1280 cm^{-1}), the rate of CF_3 vibrational relaxation should be fairly rapid. Addition of N_2O (which also has a vibrational energy level coincident with CF_3) to the photolysis mixture had no effect on either the rise time of the CF_3 signal or its peak yield. Thus, it is likely that CF_3 vibrational relaxation is near completion after about 50 μs.

Product Yield as a Function of Fluence. A number of independent data sets over a range of conditions was required to properly quantify the C_2F_6 and CO (and thus the CF_3) obtained in the IRMPD of hfa. Thus these yields were monitored in the capillary cell over a range of fluences with an initial hfa pressure of 600 mTorr. A plot of C_2F_6 yield (after CF_3 recombination is complete, about 500 μs) and CO yield (measured 100 μs after the pulse) versus fluence is given in Figure 3. As expected, the CO and C_2F_6 yields are equal within experimental error. From the stoichiometry of the dissociation, the initial CF_3 yield is twice the C_2F_6 and CO yields. Thus α_0, the CF_3 absorption at line center, can be related to twice the C_2F_6 or CO yield at each fluence studied (see Figure 4).

Before quantification can be done, it is important that the gas temperature following photolysis be known since aborption line strengths are temperature dependent. To measure this temperature, we added a small amount of N_2O to the photolysis mixture and performed transient absorption measurements on the P(45)

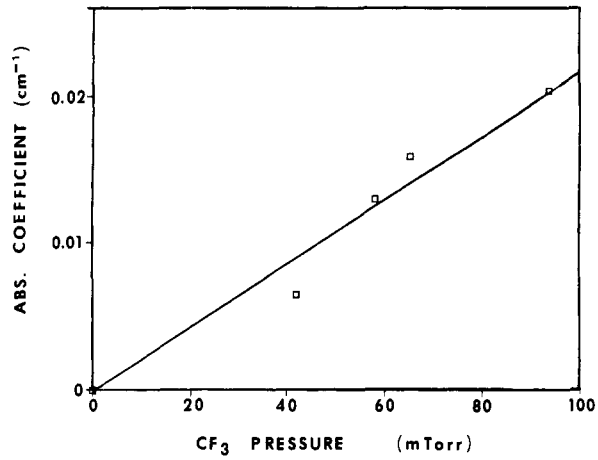

Figure 4. Plot of CF_3 absorption per centimeter at line center, α_0, as a function of CF_3 pressure. α_0 for CF_3 is measured at a variety of CO_2 laser fluences, and the CF_3 pressure is obtained from the CO and C_2F_6 yields measured at each of these fluences and a knowledge of dissociation stoichiometry.

N_2O line at 1243.795 cm^{-1} following photolysis at a fluence of 35 J cm^{-2}. No noticeable increase in N_2O absorption (within 10%) was noted over a time scale ranging from 50 μs to 20 ms, indicating no detectable temperature rise (less than 10 K) following the passage of the CO_2 laser pulse.

This lack of an observable temperature rise indicates that the activation energy for reaction 3b, suggested to be 83.1 kJ mol^{-1},[18] is provided by internal energy at the time of CF_3CO formation and/or by additional IR absorption during the laser pulse.

Line Strength and Band Strength of CF_3. The CF_3 line strength can then be obtained by using the following relation:[19]

$$\alpha_0 = (\ln 2/\pi)^{1/2}(S/\delta f_D)(P/760) \quad (5)$$

where S is the line strength, P is the pressure in Torr, and δf_D is the Doppler half-width at half-maximum (hwhm) of the transition. Thus, the slope of the α_0 versus P plot (Figure 4) is $(\ln 2/\pi)^{1/2})(S/\delta f_D)$. The Doppler hwhm for CF_3 is 9.44×10^{-4} cm^{-1}, and thus the line strength for $^rR_{16}(20)$ of CF_3 (1243.739 cm^{-1}) is determined to be $(1.4 \pm 0.3) \times 10^{-20}$ cm $molecule^{-1}$.

The measure of this single CF_3 ν_3 line strength allows the calculation of all other ν_3 line strengths as well as an estimate of the ν_3 band strength. The general line-strength formula is as follows:[19]

$$S = (8\pi^3 f/3hcp)(N/Q_vQ_r)g_{NK}R_v^2R_r^2 \exp(-(E_{NK}/kT) \times (1 - \exp(1 - hcf/kT)) \quad (6)$$

where f is the transition frequency in cm^{-1}, R_v^2 is the vibrational contribution to the transition moment, R_r^2 is the Honl–London factor, g_{NK} is the degeneracy, E_{NK} is the rotational energy of the lower level, and h, c, and p are Planck's constant, the velocity of light, and pressure, respectively.

Since only g_{NK}, R_r^2, f, and E_{NK} change with the particular line being considered, the ratio of one line strength to another can be easily determined.

The band strength A, the sum of all line strengths in the band, is

$$A = (8\pi^3 f_0/3hcp)(N/Q_v)R_v^2(1 - \exp(hcf_0/kT)) \quad (7)$$

where f_0 is the band origin.[19] If it is assumed that $f \approx f_0$, then the band strength can be obtained from a line strength from the ratio of eq 6 and 7:

$$A = [SQ_r]/[R_r^2(g_{NK}) \exp(-E_{NK}/kT)] \quad (8)$$

(18) Kerr, J. A.; Wright, J. P. *J. Chem. Soc., Faraday Trans. 1* **1985**, *81*, 1471.
(19) Penner, S. S. *Quantitative Molecular Spectrescopy and Gas Emissivities*; Addison-Wesley: Reading, MA, 1959.
(20) Selamoglu, N.; Rossi, M. J.; Golden, D. M. *Chem. Phys. Lett.* **1986**, *124*, 68.

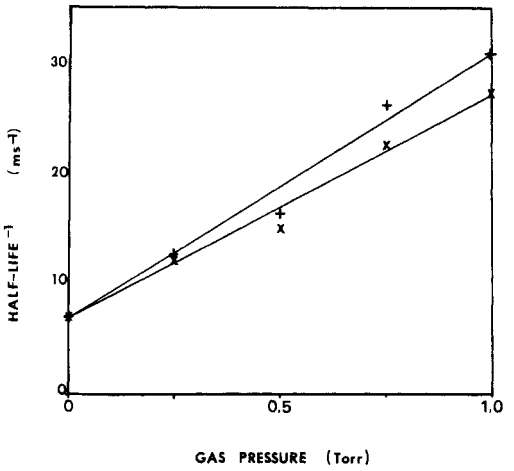

Figure 5. Plot of the inverse of the CF_3 half-life versus the NO (+) or O_2 (×) pressure. The CF_3 is created by the photolysis of 600 mTorr of hfa (in the presence of the added NO or O_2 in a 1-mm capillary cell at fluence of 35 J cm^{-2}).

With our measured line strength, the degeneracy, the Boltzmann factor for $^rR_{16}(20)$, and Q_r for CF_3, the CF_3 ν_3 band strength is determined to be $(3.2 \pm 0.8) \times 10^{-17}$ cm $molecule^{-1}$, a factor of 3 below the predicted value,[21a] a factor of 2 larger than our measured value for CF_2 ν_1,[10] and a factor of 6 smaller than that of CF_4 ν_3, one of the strongest absorptions known.

To the extent that CF_3 decays during the 50 μs after the laser pulse and before our measurement of its initial "peak" absorption intensity, our values of line strength and band strength will be too low, and one might expect an error of up to 50%. However, this effect appears to be minor, because we see no significant C_2F_6 at that stage, within an experimental error of perhaps 10%.

Absolute Reaction Kinetics. Knowledge of the line strength and hence the absolute CF_3 concentration allows a study of CF_3 reaction kinetics. In the case of pure hfa photolysis, the only reaction of CF_3 is decay via recombination (eq 3b). Thus, at constant third-body concentration

$$d/dt\ (CF_3) = -2k_4(CF_3)^2 \qquad (9)$$

and CF_3 decay should be second order, as confirmed by our observations. The rate constant for CF_3 recombination, k_4, has been determined in our previous publication[12] to be $(2.2 \pm 0.5) \times 10^{-12}$ cm^3 $molecule^{-1}$ s^{-1} at 300 K, for a hfa pressure of 600 mTorr. The high-pressure limit for reaction 4 has recently been determined to be 4×10^{-12} cm^3 $molecule^{-1}$ s^{-1}.[20] Thus it appears that with 600 mTorr of hfa as the third body, our measurements are in the falloff region, though the pressure dependence is still small.[12]

In addition, the CF_3 decay has been monitored in the presence of NO and O_2. For these cases, CF_3 decay can also occur via

$$CF_3 + 2X \rightarrow CF_3X + X \qquad (10)$$

$$CF_3 + X + M \rightarrow CF_3X + M \qquad (11)$$

where X = O_2 or NO.

Since the recombination rate cannot be neglected relative to reaction with the added gas, the analysis of Laguna and Baughcum was used:[21b]

$$(\ln 2)/t_{1/2} = k_{10}(X)^2 + k_{11}(X)(M) + (k_4/\ln 2)(CF_3)_0 \qquad (12)$$

where $(CF_3)_0$ is the initial CF_3 concentration and $t_{1/2}$ is the time at which $(CF_3) = {}^1/_2(CF_3)_0$. Figure 5 shows a plot of $1/t_{1/2}$ versus (O_2) or (NO). (The hfa pressure is constant at 600 mTorr.) In both cases, this plot gives a good straight line, whereas a plot versus $(O_2)^2$ or $(NO)^2$ is curved. We interpret this as meaning that hfa is a much better third body than either O_2 or NO, and reaction 11 dominates over (10). The slopes of these plots yield the rate constants for reaction 11, $(2.1 \pm 0.5) \times 10^{-29}$ cm^6 $molecule^{-2}$ s^{-1} in the case of X = O_2 and $(2.8 \pm 0.7) \times 10^{-29}$ cm^6 $molecule^{-2}$ s^{-1} in case of X = NO. While the rate constant for CF_3 reaction with O_2, with hfa as third body, has not been previously reported, the rate constant with M = N_2 has recently been found to be $(1.9 \pm 0.2) \times 10^{-29}$ cm^6 $molecule^{-2}$ s^{-1}.[22] This value is similar to our value with M = hfa, contrary to expectation, since N_2 is a less efficient collision partner than hfa. To the best of our knowledge the only published rate constant for the reaction of CF_3 and NO is a high-pressure-limited value of 1.6×10^{-11} cm^3 $molecule^{-1}$ s^{-1}, measured at total pressures greater than 20 Torr.[23]

Conclusions

In this paper, the IRMPD of hexafluoroacetone has been investigated, by using a time-resolved TDL absorption technique to identify and measure absolute yields of transient and stable products of the photolysis. It was found that the major dissociation pathway led to the production of CO and two CF_3 radicals, which then combine to form C_2F_6. The lack of significant yields of CF_2 or CF_4 eliminates the possibility of secondary dissociation or disproportionation of CF_3. Evidence for a second, minor, channel of dissociation, forming CF_3COF and CF_2 was found in many-pulse photolyses. The quantification of the C_2F_6 and CO formed in a single pulse allows determination of the absolute CF_3 concentration and thus a measure of the CF_3 line strength ($(1.4 \pm 0.3) \times 10^{-20}$ cm $molecule^{-1}$) and the CF_3 ν_3 band strength ($(3.2 \pm 0.8) \times 10^{-17}$ cm $molecule^{-1}$) (neglecting the question of possible underestimation if any CF_3 decays prior to the first point 50 μs after the laser pulse). In addition, the kinetics of several CF_3 reactions have been studied. The rate constant for recombination of CF_3 to form C_2F_6 was measured[12] to be $(2.2 \pm 0.5) \times 10^{-12}$ cm^3 $molecule^{-1}$ s^{-1}, while the rate constants for CF_3 reacting with O_2 and NO were found to be $(2.1 \pm 0.5) \times 10^{-29}$ and $(2.8 \pm 0.7) \times 10^{-29}$ cm^6 $molecule^{-2}$ s^{-1}, respectively.

Acknowledgment. We thank Atomic Energy of Canada Ltd. for the loan of the Lumonics TEA 801A CO_2 laser used in this work. We also thank C. E. Brown and P. H. Beckwith for their help in developing the high-frequency modulation technique and Dr. J. Reid (Department of Engineering Physics) for his general guidance in the development of the TDL techniques and for helpful discussions regarding this work. We are also grateful to the reviewers for their helpful remarks.

Registry No. $(CF_3)_2CO$, 684-16-2; CF_3, 2264-21-3; C_2F_6, 76-16-4; CO, 630-08-0; O_2, 7782-44-7; NO, 10102-43-9.

(21) (a) Newton, J. H.; Person, W. P. *J. Chem. Phys.* **1978**, *68*, 2799. (b) Laguna, G. A.; Baughcum, S. L. *Chem. Phys. Lett.* **1982**, *88*, 568.

(22) Caralp, F.; Lesclaux, R.; Dognon, A. M. *Chem. Phys. Lett.* **1986**, *129*, 433.

(23) Amphlett, J. C.; MacAuley, L. J. *Can. J. Chem.* **1976**, *54*, 1234.